17. Adler LP, Blair HF, Makley JT, et al. Noninvasive grading of musculoskeletal tumors using PET. *J Nucl Med* 1991;32:1508–1512.
18. Hoh C, Hawkins RA, Glaspy J. PET total body imaging in breast cancer with ^{18}F ion and FDG [Abstract]. *Clin Nucl Med* 1990;15:763.
19. Wahl RL, Cody R, Hutchins G, Mudgett E. Positron-emission tomographic scanning of primary and metastatic breast carcinoma with the radiolabeled glucose analog 2-deoxy-2-[^{18}F]fluoro-D-glucose [Letter]. *N Engl J Med* 1991;324:200.
20. Wahl RL, Cody RL, Hutchins GD, Mudgett EE. Primary and metastatic breast carcinoma: initial clinical evaluation with PET with the radiolabeled glucose analog 2-[^{18}F]-fluoro-2-deoxy-D-glucose. *Radiology* 1991;179:765–770.
21. Harney JV, Wahl RL, Liebert M, et al. Uptake of 2-deoxy, 2-(^{18}F) fluoro-D-glucose in bladder cancer: animal localization and initial patient positron emission tomography. *J Urol* 1991;145:279–283.
22. Francavilla TL, Miletich RS, DeMichele D, et al. Positron emission tomography of pituitary macroadenomas: hormone production and effects of therapies. *Neurosurgery* 1991;28:826–833.
23. De Souza B, Brunetti A, Fulham MJ, et al. Pituitary microadenomas: a PET study. *Radiology* 1990;177:39–44.
24. Strauss LG, Clorius JH, Schlag P, et al. Recurrence of colorectal tumors: PET evaluation. *Radiology* 1989;170:329–332.
25. Yonekura Y, Benua RS, Brill AB, et al. Increased accumulation of 2-deoxy-2-[^{18}F]fluoro-D-glucose in liver metastases from colon carcinoma. *J Nucl Med* 1982; 23:1133–1137.
26. Okazumi S, Isono K, Enomoto K, et al. Evaluation of liver tumors using fluorine-18-fluorodeoxyglucose PET: characterization of tumor and assessment of effect of treatment. *J Nucl Med* 1992;33:333–339.
27. Joensuu H, Ahonen A. Imaging of metastases of thyroid carcinoma with fluorine-18-fluorodeoxyglucose. *J Nucl Med* 1987;28:910–914.
28. Francavilla TL, Miletich RS, Di CG, Patronas NJ, Rizzoli HV, Wright DC. Positron emission tomography in the detection of malignant degeneration of low-grade gliomas. *Neurosurgery* 1989;24:1–5.
29. Alavi JB, Alavi A, Chawluk J, et al. Positron emission tomography in patients with glioma: a predictor of prognosis. *Cancer* 1988;62:1074–1078.
30. Schlag P, Lehner B, Strauss LG, Georgi P, Herfarth C. Scar or recurrent rectal cancer. Positron emission tomography is more helpful for diagnosis than immunoscintigraphy. *Arch Surg* 1989;124:197–200.
31. Minn H, Paul R, Ahonen A. Evaluation of treatment response to radiotherapy in head and neck cancer with fluorine-18-fluorodeoxyglucose. *J Nucl Med* 1988;29:1521–1525.
32. Minn H, Paul R. Cancer treatment monitoring with fluorine-18 2-fluoro-2-deoxy-D-glucose and positron emission tomography: frustration or future [Editorial]. *Eur J Nucl Med* 1992;19:921–924.
33. Hawkins RA, Choi Y, Huang SC, Messa C, Hoh CK, Phelps ME. Quantitating tumor glucose metabolism with FDG and PET [Editorial]. *J Nucl Med* 1992;33:339–344.
34. Lammertsma AA, Brooks DJ, Frackowiak RS, et al. Measurement of glucose utilization with [^{18}F]2-fluoro-2-deoxy-D-glucose: a comparison of different analytical methods. *J Cereb Blood Flow Metab* 1987;7:161–172.
35. Fischman AJ, Alpert NM. FDG-PET in oncology: there's more to it than looking at pictures [Editorial]. *J Nucl Med* 1993;34:6–11.
36. Graham MM, Lewellen TK. Positron emission tomography and its role in metabolic imaging. *Mayo Clin Proc* 1989;64:725–727.
37. Kim CK, Gupta NC, Chandramouli B, Alavi A. Standardized uptake values of FDG: body surface area correction is preferable to body weight correction [see comments]. *J Nucl Med* 1994;35:164–167.
38. Langen KJ, Braun U, Kops RE, et al. The influence of plasma glucose levels on fluorine-18-fluorodeoxyglucose uptake in bronchial carcinomas. *J Nucl Med* 1993;34: 355–359.
39. Lindholm P, Minn H, Leskinen-Kallio S, Bergman J, Ruotsalainen U, Joensuu H. Influence of the blood glucose concentration on FDG uptake in cancer—a PET study. *J Nucl Med* 1993;34:1–6.
40. Hamberg LM, Hunter GJ, Alpert NM, Choi NC, Babich JW, Fischman AJ. The dose uptake ratio as an index of glucose metabolism: useful parameter or oversimplification? *J Nucl Med* 1994;35:1308–1312.
41. Kilbourn MR, Hood JT, Welch MJ. A simple ^{18}O-water target for ^{18}F production. *Int J Appl Radiat Isot* 1984;35:599–602.
42. Hamacher K. Phase-transfer catalyzed synthesis of 4-S-β D-glucopyranosyl-2-thio-D-glucopyranose (thiocellobiose) and 2-S-β D-glucopyranosyl-2-thio-D-glucopyranose (thiosophorose). *Carbohydr Res* 1984;27:291–295.
43. Hamacher K, Coenen HH, Stocklin G. Efficient stereospecific synthesis of no-carrier-added 2-[^{18}F]-fluoro-2-deoxy-D-glucose using aminopolyether supported nucleophilic substitution. *J Nucl Med* 1986;27:235–238.
44. Rota KE, Herzog H, Schmid A, Holte S, Feinendegen LE. Performance characteristics of an eight-ring whole body PET scanner. *J Comput Assist Tomogr* 1990;14:437–445.
45. Phelps ME, Huang SC, Hoffman EJ, Selin C, Sokoloff L, Kuhl DE. Tomographic measurement of local cerebral glucose metabolic rate in humans with [^{18}F]2-fluoro-2-deoxy-D-glucose: validation of method. *Ann Neurol* 1979;6:371–388.
46. Rhodes CG, Wise RJ, Gibbs JM, et al. In vivo disturbance of the oxidative metabolism of glucose in human cerebral gliomas. *Ann Neurol* 1983;14:614–626.
47. Guyton AC. Chapter 25. The body fluid compartments: extracellular and intracellular fluids; interstitial fluid and edema. In: *Textbook of medical physiology*, 8th ed. Philadelphia: W.B. Saunders; 1991:273–285.
48. Keyes JW, Harkness BA, Greven KM, Williams DW, Watson NE, McGuirt F. Pretherapy evaluation with PET of salivary tumors [Abstract]. *Radiology* 1993; 147(suppl):189P.
49. Inoue T, Kim EE, Komaki R, et al. Detecting recurrent or residual lung cancer with FDG-PET. *J Nucl Med* 1995;36:788–793.
50. Lowe VJ, DeLong DM, Hoffman JM, Coleman RE. Optimum scanning protocol for FDG-PET evaluation of pulmonary malignancy. *J Nucl Med* 1995;36:883–887.
51. Gupta NC, Chandramouli B, Frank A, Dewan N, Scott W. PET FDG imaging for estimating probability of malignancy in solitary pulmonary nodules [Abstract]. *Radiology* 1993;147(suppl):189P.
52. Gupta N, Dewan N, Frank A, Mailliard J, Scott W. Presurgical evaluation of patients with suspected malignant pulmonary nodules using PET-FDG imaging [Abstract]. *J Nucl Med* 1993;34(suppl):20P.
53. Haberkorn U, Strauss LG, Dimitrakopoulou A, et al. Fluorodeoxyglucose imaging of advanced head and neck cancer after chemotherapy. *J Nucl Med* 1993;34:12–17.

Thallium-201 Uptake, Histopathological Differentiation and Na-K ATPase in Lung Adenocarcinoma

Hironori Takekawa, Kazuo Itoh, Shosaku Abe, Shigeaki Ogura, Hiroshi Isobe, Masayori Furudate and Yoshikazu Kawakami

First Department of Medicine and Department of Nuclear Medicine, School of Medicine, Hokkaido University; and Third Department of Medicine, School of Medicine, Sapporo Medical University, Sapporo, Japan

To clarify differences in accumulation in ^{201}Tl scintigraphy, we examined the relationship between uptake of ^{201}Tl, histopathological differentiation and Na-K ATPase. **Methods:** Thallium-201 SPECT was performed twice: 15 min (early scan) and 120 min (delayed scan) after intravenous injection of 3 mCi ^{201}Tl-chloride. The uptake ratio of ^{201}Tl was calculated and compared with the grade of differentiation and the staining pattern of Na-K ATPase. **Results:** The sensitivity of ^{201}Tl SPECT for well-differentiated adenocarcinomas was lower than that for moderately and poorly differentiated ones. The uptake ratio on the delayed scan was significantly lower in the well-differentiated group than that in the moderately and poorly differentiated groups. This parameter was also significantly higher in the Na-K ATPase-positive group than the -negative group. **Conclusions:** These results indicate that the uptake ratio of ^{201}Tl SPECT may be a noninvasive indicator of the grade of pathological differentiation of adenocarcinoma and provide insight into the relationship among ^{201}Tl SPECT, malignancy and Na-K ATPase.

Key Words: thallium-201 single-photon emission computed tomography; grade of differentiation; Na-K ATPase; adenocarcinoma of the lung

J Nucl Med 1996; 37:955–958

Received Apr. 17, 1995; revision accepted Sept. 7, 1995.

For correspondence or reprints contact: Hironori Takekawa, MD, Department of Respiratory Medicine, Nikko Memorial Hospital, 1-5-13 Shintomi-cho, Muroran 051, Japan.

Thallium-201 scintigraphy is widely used in the diagnosis of myocardial infarction (*1*), myocardial ischemia (*2*), thyroid tumors (*3,4*), head and neck cancer (*5*) and bone and soft-tissue sarcoma (*6*). For lung cancer, ^{201}Tl SPECT has a higher sensitivity than ^{67}Ga scintigraphy (*7–9*).

Thallium-201 accumulation on early and delayed scans differs between benign and malignant tumors (*3,4,7,10*). In malignant tumors, ^{201}Tl accumulation was seen on both early and delayed scans but not on delayed scans of benign tumors. Retention of ^{201}Tl on delayed scans is strongly suggestive of malignancy; however, the mechanism of this difference in accumulation pattern remains unknown at present.

In thyroid cancer, Ochi et al. (*3*) reported that ^{201}Tl was strongly positive on all early and delayed scans of anaplastic carcinoma and was strongly positive on early scans and weakly positive or negative on delayed scans in 37% (10 of 27) of papillary and follicular carcinomas. Our preliminary studies showed that some well-differentiated adenocarcinomas of the lung were positive on the early scan and negative on the delayed scan. These data suggest that the degree of accumulation of ^{201}Tl on the delayed scan might be associated with histopathological differentiation.

Influx of ^{201}Tl into malignant cells is regulated by the active transport of Na-K ATPase (*11–13*). In ^{201}Tl scintigraphy, ^{201}Tl accumulation might be closely correlated with the Na-K ATPase levels of malignant tumors (*11,12*).

To clarify the difference in accumulation on both early and delayed scans in ^{201}Tl scintigraphy, we examined the relationship among the grade of histopathological differentiation, Na-K ATPase staining and uptake of ^{201}Tl in adenocarcinoma of the lung.

MATERIALS AND METHODS

Patients

Thallium-201 SPECT studies were performed in 55 patients (28 men, 27 women; aged 37–79 yr; mean [±s.d.] age 59.6 ± 11.0 yr) with adenocarcinoma of the lung at our hospital from 1990 to 1994. Diagnosis was made by histopathological analysis of endoscopic samples, lobectomy or pneumonectomy. Each patient gave informed consent.

Imaging

Thallium-201 SPECT scans were acquired twice: 15 min (early scan) and 120 min (delayed scan) after an intravenous injection of 3 mCi (111 MBq) of ^{201}Tl-chloride. A gamma camera (GE-Maxi 400AT/C) equipped with a general-purpose parallel-hole collimator was interfaced with a dedicated computer (Starcom II). The detector focusing on the chest was rotated in stages of approximately 6 degrees for a total of 360°. Image data was collected for 30 sec at each stop. Transaxial images were reconstructed with a Hanning prefilter and a Ramp postfilter. Coronal and sagittal section images were assembled from transaxial images (*9*). Without prior knowledge of the cytological or pathological findings, all the images were interpreted for the presence or absence of abnormal accumulation by two nuclear medicine specialists (K.I.,M.F.).

When the ^{201}Tl SPECT scan showed abnormal uptake in the primary lesion of the lung cancers, regions of interest (ROIs) were assigned for the areas with abnormal radioactivity and the contralateral normal lung on the coronal sections of both the early and delayed scans. The mean pixel counts for the ROIs were measured, and the uptake ratios between the lesion and the contralateral normal lung were calculated for both the early and the delayed scans.

Adenocarcinomas of the lung were subgrouped into well-, moderately and poorly differentiated carcinomas according to the World Health Organization classification of lung tumors (*14*).

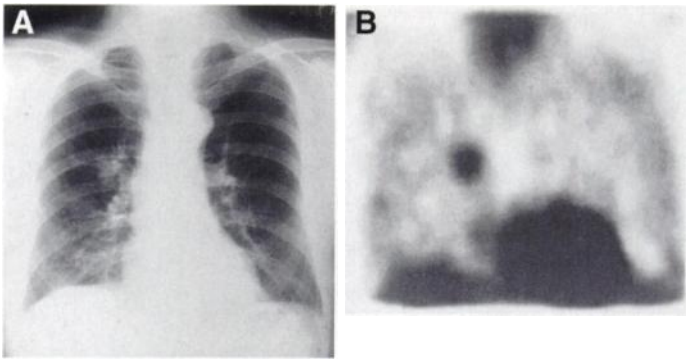

FIGURE 1. Images from a 74-yr-old woman with lung carcinoma. (A) Plain chest radiograph showing a pulmonary nodule in the right upper lung field. (B) Transaxial ^{201}Tl SPECT image from delayed scan showing a round focal accumulation in the right upper field of the chest.

Immunostaining

Immunostaining of Na-K ATPase was by a monoclonal antibody against purified human renal Na-K ATPase, provided by BYK Pharmaceuticals (Konstanz, Germany). The immunostaining was performed using avidin-biotin peroxidase complex technique (Vectastain, Vector Laboratories). Sections embedded in paraffin were deparaffinized in xylol and rehydrated in a graded alcohol series with distilled water. The sections were incubated in 3% H_2O_2 for 10 min to block the activity of endogenous peroxidase, washed three times for 5 min with phosphate-buffered saline (PBS) and incubated overnight at 4°C with the Na-K ATPase antibody. Color was developed with 0.05% diaminobezidine and 0.01% H_2O_2 in PBS for 5 min at room temperature. The nuclei were stained with Mayer hematozylin. Finally, the sections were washed with distilled water, dehydrated and mounted. The immunoreactivity of Na-K ATPase was classified into three groups as follows: *low-grade expression* (Na-K ATPase [−]) = staining of 0%–19% of the cancer cells; *intermediate-grade expression* (Na-K ATPase [±]) = staining of 20%–79% of the cancer cells; *high-grade expression* (Na-K ATPase[+]) = staining of 80%–100% of the cancer cells. Immunostaining of Na-K ATPase was performed in specimens available from the 14 patients who underwent operation.

Statistical Analysis

Between-group comparisons were done with the Mann-Whitney U-test. Differences were considered significant at $p < 0.05$.

RESULTS

In 55 adenocarcinomas, the sensitivity was 93% (51 of 55) on the early scan and 89% (49 of 55) on the delayed scan (Fig. 1). Negative results on ^{201}Tl SPECT included five well-differentiated and one moderately differentiated adenocarcinoma as defined by histological differentiation. Lesions that were not detected on ^{201}Tl SPECT were 1.4, 1.5, 1.9, 2.1, 2.4 and 3.0 cm in diameter. The minimum lesion size detected on ^{201}Tl SPECT was 1.5 cm. Seven adenocarcinomas between 1.5 and 2.0 cm and 15 between 2.1 and 3.0 cm were detected, resulting in a sensitivity of 70% (7 of 10) for tumors between 1.4 and 2.0 cm and 83% for tumors between 2.1 and 3.0 cm. In 29 adenocarcinomas with pathologically confirmed differentiation, the sensitivity on the delayed scan was 64% (9 of 14) for well-differentiated, 83% (5 of 6) for moderately differentiated and 100% (9 of 9) for poorly differentiated adenocarcinomas. Thus, histological differentiation was associated with sensitivity of ^{201}Tl SPECT in adenocarcinoma of the lung.

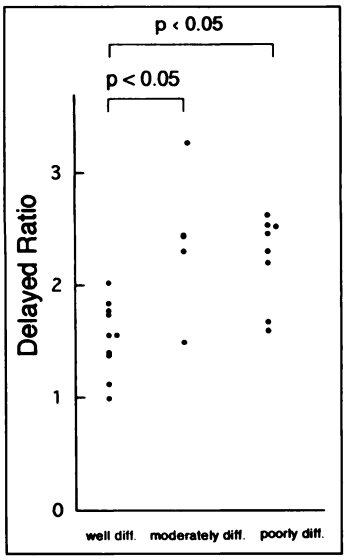

FIGURE 2. Correlation of grade of differentiation (diff.) and delayed ratios in adenocarcinoma of the lung.

Figure 2 shows the delayed ratios compared with the grade of differentiation. In 22 adenocarcinomas with both confirmed histological differentiation and uptake ratio of ^{201}Tl SPECT, the delayed ratios were significantly lower in the well-differentiated group ($n = 10$) than the moderately ($n = 4$) and poorly ($n = 8$) differentiated groups ($p < 0.05$).

In primary tumor tissues, immunoperoxidase reactivity to Na-K ATPase was present in the cytoplasm of some of the cancer cells (Fig. 3). In normal tissues, the cilia of the epithelium in the bronchi were strongly stained using this method. Figure 4 shows the delayed ratios between the Na-K ATPase-positive and -negative groups in adenocarcinoma of the lung. The delayed ratios were significantly higher in the Na-K ATPase-positive group ($n = 8$) than in the -negative group ($n = 6$) ($p < 0.05$).

DISCUSSION

This study demonstrated a close relationship among the grade of pathological differentiation, the grade of Na-K ATPase staining and the uptake ratios of ^{201}Tl SPECT in adenocarcinoma of the lung. The sensitivities of ^{201}Tl SPECT to adenocarcinoma of the lung were related to its histopathological differentiation. In well-differentiated adenocarcinoma, the uptake ratios on the delayed ^{201}Tl SPECT scans were significantly lower than in both moderately and poorly differentiated adenocarcinomas. This relationship might be associated with Na-K ATPase, because the uptake ratios on the delayed ^{201}Tl SPECT scans were also associated with the intensities of the Na-K ATPase staining. Our results suggest that ^{201}Tl SPECT may predict the differentiation of the adenocarcinoma and estimate the prognosis. The grade of differentiation is one of the factors determining the survival of patients with adenocarcinoma of the lung. Saijo et al. (*15*) reported that among 119 patients survival of those with well-differentiated adenocarcinoma was significantly greater than that in those with poorly differentiated adenocarcinoma. We reported that in an adenocarcinoma with lymph node metastasis, ^{201}Tl demonstrated slow washout or increased retention on the delayed scan (*16*). We also observed that uptake on the delayed scan was associated with lymph node metastasis and the grade of differentiation in adenocarcinoma of the lung. This finding accounts for the higher frequency of lymph node metastasis in poorly differentiated adenocarcinoma (*17*).

The accumulation patterns of ^{201}Tl on early and delayed scans differ between benign and malignant lung and thyroid tumors (*3,4,18*). In malignant tumors, ^{201}Tl may show different accumulation in relation to the grade of histopathological differentiation. In supratentorial gliomas, the ^{201}Tl index, expressed as the ratio of count rate of the tumor site to the count rate over the contralateral normal region, was significantly higher in patients with grade IV glioma than in those with lower grade glioma (*19*). We showed that the delayed ratio of ^{201}Tl SPECT was associated with the grade of differentiation and Na-K ATPase in adenocarcinoma of the lung.

On ^{201}Tl scintigraphy, the early ratio in a tumor reflected the angiographic vascularity (*20*) and blood pooling (*21*). The delayed ratio reflected the cell's ability to pick up ^{201}Tl (*21,22*) or histological cellularity (viability of tumor cells) (*11,23*).

Thallium is a potassium analog because it, as well as potassium, is a metallic element in group 3-A of the periodic table. It has five times the affinity to the cell as potassium. Thus, thallium is transported into cells instead of potassium. This transportation might be related to Na-K ATPase. This speculation is supported by an in vitro experiment that demonstrates that the active transport of thallium into malignant cells is regulated by Na-K ATPase (*8,11,12*). In the present study, we showed that the delayed ratios of the positive tumors in immunohistochemical staining for Na-K ATPase were significantly higher than those of the negative tumors. Thus, uptake of ^{201}Tl on the delayed scan might be regulated by Na-K ATPase in adenocarcinoma of the lung.

In cultured cells, the activity of Na-K ATPase in the transformed cell was elevated compared with that in the parent normal cell. This finding accounts for synthesis of the enzyme halting in normal cells or for increased Na-K ATPase before cell division in the transformed cell (*24*). This indicated that the differentiation might be associated with Na-K ATPase and uptake of ^{201}Tl. Thyroid cancer tissue has higher activity levels of Na-K ATPase than normal thyroid tissue (*12*), which means that Na-K ATPase may be associated with ^{201}Tl uptake in thyroid cancer. We showed that in adenocarcinoma of the lung, ^{201}Tl uptake on the delayed scan was related to the differentiation and intensity of the Na-K ATPase staining.

CONCLUSION

The uptake ratio of the delayed scan on ^{201}Tl SPECT is related to the grade of histopathological differentiation in adenocarcinoma of the lung. This is associated with the degree of the Na-K ATPase expression. Thus, this ratio is a useful indicator of the grade of histopathological differentiation,

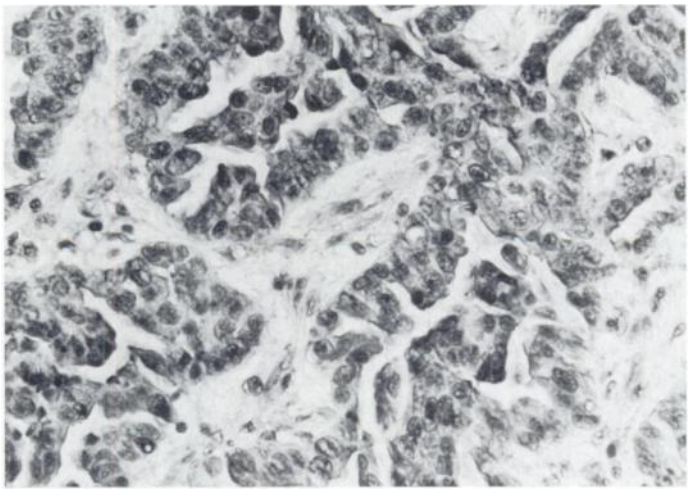

FIGURE 3. Immunohistochemical staining of lung cancer with anti-Na-K ATPase antibody. High-grade expression (Na-K ATPase [+]) in adenocarcinoma of the lung. Original magnification ×200.

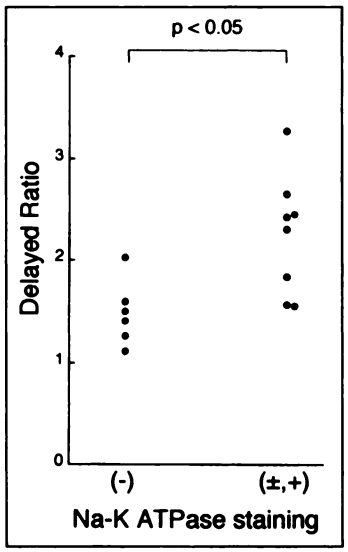

FIGURE 4. Correlation of Na-K ATPase and delayed ratios in adenocarcinomas of the lung.

thereby facilitating the prediction of prognosis, and provides insight into the relationship between ^{201}Tl uptake and malignancy.

REFERENCES

1. Strauss HW, Harrison K, Langan JK, Lebowitz E, Pitt B. Thallium-201 for myocardial imaging: relation of thallium-201 to regional myocardial perfusion. *Circulation* 1975;51:641–645.
2. Strauss HW, Boucher CA. Myocardial perfusion studies: lessons from a decade of clinical use. *Radiology* 1986;160:577–584.
3. Ochi H, Sawa H, Fukuda T, Inoue Y, Nakajima H. Thallium-201-chloride thyroid scintigraphy to evaluate benign and/or malignant nodules. *Cancer* 1982;50:236–240.
4. El-Desouki M. Thallium-201 thyroid imaging in differentiating benign from malignant thyroid nodules. *Clin Nucl Med* 1991;16:425–430.
5. El-Gazzar AH, Sahweil A, Abdel-Rahim SM. Experience with thallium-201 scintigraphy. *Clin Nucl Med* 1988;13:159–165.
6. Ramanna L, Waxman AM, Waxman S. Thallium-201 scintigraphy in bone and soft-tissue sarcoma: evaluation of tumor mass and viability [Abstract]. *J Nucl Med* 1988;29:854.
7. Tonami N, Shuke N, Yokoyama K, et al. Thallium-201 single photon emission computed tomography in the evaluation of suspected lung cancer. *J Nucl Med* 1989;30:997–1004.
8. Matsuno S, Tanabe M, Kawasaki Y, et al. Effectiveness of planar image and single photon emission tomography of thallium-201 compared with gallium-67 in patients with primary lung cancer. *Eur J Nucl Med* 1991;19:86–95.
9. Itoh K, Takekawa H, Tsukamoto E, et al. Single photon emission computed tomography using ^{201}Tl-chloride in pulmonary nodules: comparison with ^{67}Ga-citrate and ^{99m}Tc-labeled hexamethl-propleneamine-oxime. *Ann Nucl Med* 1992;6:253–260.
10. Suga K, Kume N, Orihashi N, et al. Difference in ^{201}Tl accumulation on single photon emission computed tomography in benign and malignant lesions. *Nucl Med Commun* 1993;14:1071–1078.
11. Sehweil AM, McKillop JH, Milroy R, Wilson R, Abdel-Dayem HM, Omar YT. Mechanism of ^{201}Tl uptake in tumors. *Eur J Nucl Med* 1989;15:376–379.
12. Kishida T. Mechanisms of thallium-201 accumulation to thryoid gland. *Kaku Igaku* 1987;24:991–1004.
13. Muranaka A. Accumulation of radioisotopes with tumor affinity II. Comparison of the tumor accumulation of ^{67}Ga-citrate and ^{201}Tl-chloride in vitro. *Acta Med Okayama* 1981;35:85–101.
14. World Health Organization. *Histological typing of lung tumors.* 2nd ed. Geneva: World Health Organization; 1981:25–26.
15. Saijo N, Niitani H, Tominaga K. Comparison of survival in nonresected well differentiated and poorly differentiated adenocarcinoma of the lung. *J Cancer Res Clin Oncol* 1980;97:71–79.
16. Takekawa H, Itoh K, Abe S, et al. Retention index of thallium-201 SPECT as an indicator of metastasis in adenocarcinoma of the lung. *Br J Cancer* 1994;70:315–318.
17. Takise A, Kodama T, Shimosato Y, Watanabe S, Suemasu K. Histopathologic prognostic factors in adenocarcinomas of the peripheral lung less than 2 cm in diameter. *Cancer* 1988;61:2083–2088.
18. Tonami N, Michigishi T, Bunko H. Clinical tumor scanning with ^{201}Tl-chloride. *Radioisotopes* 1976;25:829–831.
19. Oriuchi N, Tamura M, Shibazaki T, et al. Clinical evaluation of thallium-201 SPECT in supratentorial gliomas: relationship to histologic grade, prognosis and proliferative activities. *J Nucl Med* 1993;34:2085–2089.
20. Taguchi A. Clinical significance of thallium-201 single-photon emission computerized tomography (Tl-201 SPECT) in the evaluation of viability of gliomas. *Kurume Med J* 1992;39:267–278.
21. Caluser C, Macapinlac H, Healey J, et al. The relationship between thallium uptake, blood flow and blood-pool activity in bone and soft-tissue tumors. *Clin Nucl Med* 1992;17:565–572.
22. Ando A, Ando I, Katayama M. Biodistribution of ^{201}Tl in tumor bearing animals and inflammatory lesion induced animals. *Eur J Nucl Med* 1987;12:567–572.
23. Mountz JM, Raymond PA, Mckeeve PE, et al. Specific localization of thallium 201 in human high-grade astrocytoma by microautoradiography. *Cancer Res* 1989;49:4053–4056.
24. Elligsen JD, Thompson HEF, Kruuv J. Correlation of (Na-K)-ATPase activity with growth of normal and transformed cells. *Exp Cell Res* 1974;87:233–240.

Ultrasound-Guided Internal Radiotherapy Using Yttrium-90-Glass Microspheres for Liver Malignancies

Jia-He Tian, Bai-Xuan Xu, Jin-Ming Zhang, Bao-Wei Dong, Ping Liang and Xiang-Dong Wang

Departments of Nuclear Medicine and Ultrasound, The Great Wall Hospital, Beijing, China

Treatment of liver malignancies, in particular hepatocellular carcinoma, remains a serious problem because of the difficulty of delivering adequate therapeutic agents to the lesions while sparing the surrounding normal tissue. In an attempt to overcome this obstacle, intratumoral injection of ^{90}Y, a beta-emitter, was performed. **Methods:** Twenty-seven hepatocellular carcinoma's and six liver metastases were studied, most of which had failed other therapeutic modalities. Guided by ultrasound, ^{90}Y-glass microspheres (GMS) were carefully injected into predetermined tumor sites. The procedure was repeated at 3–4-wk intervals where indicated. Echographic, clinical and laboratory follow-up was conducted at regular intervals. **Results:** Twelve to 32 mo after treatment, 27 patients were still alive, with dramatic improvement of their clinical condition: 90.6% of the tumor foci became smaller, with echogenic or blood flow changes on liver sonograms. Serum titers of alpha-FP in 10 of 13 patients returned to normal levels. Repeat biopsy in nine patients showed complete tumor destruction in eight. Six patients died of either end-stage disease or wide dispersion of the tumor. **Conclusion:** The intratumoral administration of ^{90}Y-GMS under ultrasound guidance yielded a higher cure rate for liver malignancy with no severe side effects. The higher radiation dosage delivered by injected ^{90}Y to the periphery of the lesions (up to 28,215–75,720 cGy) was thought to account for the successful outcome. These results show that intratumoral radionuclide injection is feasible for treatment of malignant lesions inside the body.

Key Words: yttrium-90-glass microspheres; radionuclide therapy; liver malignancy; intratumoral delivery

J Nucl Med 1996; 37:958–963

Received Apr. 6, 1995; revision accepted Aug. 17, 1995.

For correspondence or reprints contact: Jia-He Tian, MD, Department of Nuclear Medicine, The Great Wall Hospital, Beijing, China 100853.